

Water Bath Calorimetry (120420): Report

M. Nansteel (December, 2020)

Summary

Two water bath calorimetric experiments were observed on December 4, 2020 at BLP, Cranbury. These tests featured the operation of a low-voltage plasma in cylindrical Cr-Mo steel plasma cells. The plasma formed between a tungsten electrode and a jet of liquid gallium metal, and was maintained by a DC voltage differential less than 35 V. The present tests featured significantly higher operating temperature compared to similar tests conducted on November 10, 2020. The energy released by the plasma was determined from sensible heating of the bath as well as a measurement of the mass of water boiled off and various other energy effects including electrical energy input and thermal losses from the bath. The plasma energy release was calculated using a rigorous statement of energy conservation. The present document provides a detailed description of the test apparatus, conditions and procedures used in the tests, the energy balance formulas applied in the calorimetric evaluation, and analysis of the test data to obtain the plasma energy release.

The calorimetric tests encompassed two phases. In the preheating phase the cell temperature was increased to greater than 400°C and the water bath temperature to very near 100°C. This was followed by the power phase in which power and energy flows were carefully measured in order to determine the plasma energy release. The mass of bath water lost by boiling during the preheat phase was determined from a control experiment in which conditions closely matched conditions during the preheat phase. This is a key feature of the present calorimetric method.

Two calorimetric tests were conducted on December 4, denoted here as Run 1 and Run 2. The test conditions were similar in these tests except that in Run 2 a glow discharge was operated in the cell with a voltage of about 310 V, whereas no discharge existed in Run 1. During the power phase, very vigorous boiling was observed on the outer surface of the cell suggesting a high rate of heat rejection to the bath. In each test the plasma energy release E_{Plasma} clearly exceeded the electrode energy input E_{Elect} required to maintain the plasma. Plasma performance in the two tests is summarized below

Run 1: $E_{\text{Elect}} = 6951 \text{ kJ}$; $E_{\text{Plasma}} = 9313 \text{ kJ}$; $P_{\text{Plasma}} = 55.8 \text{ kW}$; Gain = 2.34
Run 2: $E_{\text{Elect}} = 7800 \text{ kJ}$; $E_{\text{Plasma}} = 18,592 \text{ kJ}$; $P_{\text{Plasma}} = 93.0 \text{ kW}$; Gain = 3.38

where

$$\text{Gain} = \frac{E_{\text{Plasma}} + E_{\text{Elect}}}{E_{\text{Elect}}}$$

The observed gains indicate that the plasma energy is 134% and 238% of the electrical energy required to maintain the plasma in these tests.

In the measurement of plasma energy, the largest contribution to the energy balance is the energy due to vaporization of the mass δm_w of bath water. The measurement of δm_w was subject to about $\pm 0.1 \text{ kg}$ uncertainty which carried through the energy balance calculation, but resulted in less than a 2.5% change in the plasma energy release. Another factor which contributed to the uncertainty of the results is the energy loss from the bath to the laboratory by sensible cooling. This loss was estimated, very roughly, from bath cooling data gathered in a

supplemental experiment. The uncertainty in plasma energy release corresponding to the $\pm 50\%$ uncertainty in this loss was also less than 2.5%.

Critical data collected in the four calorimetric tests conducted on 11/10/20 and 12/04/20 are tabulated in Table S1. This table features the time duration of the power phase in each test as well as the average cell temperature and the approximate glow discharge voltage, current and power, as well as performance data such as plasma energy, power and gain. For the present two tests (performed on 12/04/20) the plasma performance in Run 2 far exceeded the performance in Run 1. The operating conditions, such as run duration and cell temperature, were similar for these tests, however, Run 2 was conducted with the benefit of a 310 V glow discharge, whereas there was no discharge in Run 1. Also, comparing the tests performed on 11/10/20 with those on 12/04/20, it is clear from Table S1 that plasma performance was significantly greater in the December tests, in terms of both plasma power and gain. One major difference between these two test series was the greater run duration used in the November tests. Although, this factor probably cannot explain the difference in power and gain because these performance measures are mostly independent of test duration. The other obvious difference in test conditions for the two test groups is the average cell temperature during the power phase. In the November tests this was less than 200°C and in the December tests it exceeded 400°C. This increase in operating temperature might be due, in part, to the insulating effect of the composite cell liner used in the later tests. In any case, from the limited data in Table S1 it appears that increased cell temperature and glow discharge voltage may be factors which enhance plasma performance. However, additional testing is required to further support this speculation.

Table S1. Summary of results in calorimetric tests: 11/10/20 and 12/04/20

		Δt [s]	T_{Cell} [°C]	V_{GD} [V]	I_{GD} [A]	P_{GD} [W]	δm_w [kg]	E_{Plasma} [kJ]	E_{Elect} [kJ]	Gain	P_{Plasma} [kW]
11/10/20	Run 1	302	196	220	2.04	449	6.02	6134	10,346	1.59	20.3
	Run 2	296	177	193	2.04	394	6.92	9367	9341	2.00	31.6
12/04/20	Run 1	167	458	0	0	0	7.1	9313	6951	2.34	55.8
	Run 2	200	425	310	0.38	118	11.5	18,592	7800	3.38	93.0

Background

Two calorimetric tests were observed on December 4, 2020 at BLP, Cranbury. These tests were conducted in order to measure the plasma energy release from a cylindrical Cr-Mo steel reactor cell. The cell was operated in a water bath in order to capture and measure as much of the energy release as possible. The tests were conducted with significantly higher cell temperature than the otherwise similar tests observed on November 10, 2020. Higher temperature was achieved in the present tests due to a three-piece carbon/niobium/tungsten liner which partially insulated the liquid gallium from the cooler cell wall, and also by increasing the heating intensity during the preheat phase. These modifications resulted in cell temperature at or greater than 400°C at the start of the power phase. This greatly exceeds the approximately 200°C cell temperature present during the power phase in the tests conducted on November 10. The higher cell temperatures and increased test duration resulted in increased bath temperatures and bath water boil-off. In order to accurately measure the energy related to water boil-off in the preheat phase, a separate control experiment was conducted to simulate this phase. This control experiment is a key feature of the present calorimetric method.

This document includes description of the test apparatus and conditions, documentation of the energy conservation formula applied in the calorimetric measurement, and analysis of the test data to obtain the plasma energy release.

Plasma cell description

The main part of the plasma cell is comprised of a vertical chrome-molybdenum steel tube with 8 inch OD and 0.05 inch wall thickness. A supplemental cylindrical chamber, made from a 4 inch OD chrome-molybdenum tube, also with 0.05 inch wall, is welded to the main chamber as shown in Fig. 1. The two-cylinder cell is partially filled with about 6 kg of liquid gallium which is recirculated through a stainless tube by an electromagnetic pump, resulting in a vertical jet of liquid metal as sketched in Fig. 1. The plasma is formed by a low DC voltage which is maintained between the gallium jet and a tungsten electrode extending downward into the cell from above. The cell wall is shielded from the plasma by a three-piece liner consisting of concentric layers of carbon, Nb and W, ranging in thickness from ~3-4 mm each, and radially spaced by about the same amount. The spaces between the layers trap stagnant gallium, hence reducing convection transfer to the cooler cell wall. This partially insulates the gallium from the wall and thereby increases cell temperature. The internal temperature of the cell is measured by a K-type ungrounded thermocouple probe (not shown in Fig. 1) immersed in the liquid gallium.

Either pure hydrogen flows through the cell and is then evacuated, or hydrogen is mixed with trace oxygen and reacted outside the cell and the bath before flowing through the cell, as shown in Fig. 1. Also, a vertical tube fitted with an electrode is attached to the upper flange of the cell

so that a glow discharge can be maintained there. Ionization of the hydrogen gas flow, resulting from the glow discharge process, is thought to be a key feature of the plasma reaction.

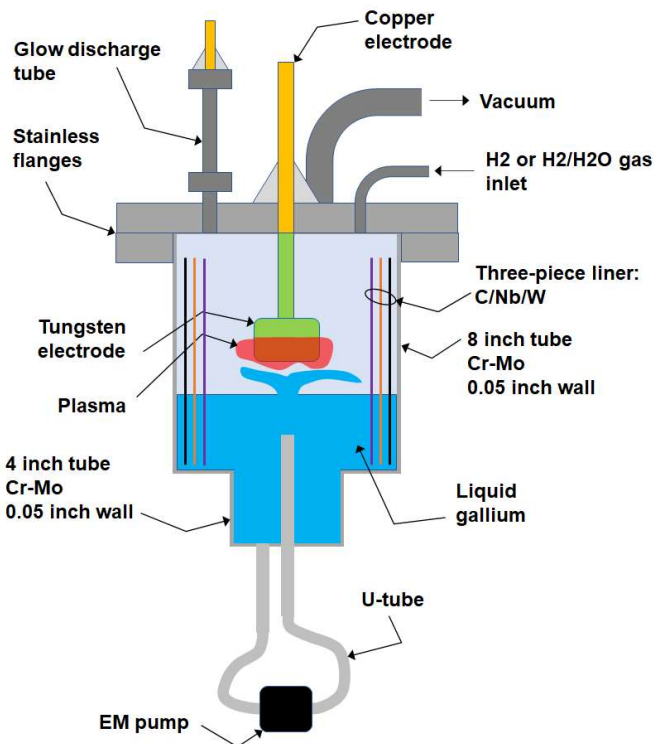


Figure 1. Schematic diagram of plasma cell with three-piece liner

Calorimetric measurement procedure

The calorimetric measurement of plasma energy is achieved in a two-phase process. First, a preheating phase with variable electric power input and plasma heat release is used to heat the cell to near 400°C and the bath water up to the boiling temperature. In the later stages of this preheat phase the electrode power input is increased and the glow discharge is deployed with hydrogen and trace water vapor flow through the cell to further preheat both the cell and the bath. During the subsequent power phase these conditions are maintained while the relevant power inputs, the bath temperature rise, and vaporization losses are carefully measured so that an accurate calorimetric estimate of the plasma heat release is possible.

System tank

The plasma cell is fixtured in a cylindrical plastic tank, denoted here as the system tank. This tank is 1/8 inch thick HDPE with 22 inch diameter and 36 inch height. The tank is well insulated around its circumference and over its lower surface. Also installed in the system tank are two water jet pumps as well as the various cell support structure components, power cables, and gas

feed and vacuum lines. The system tank is initially dry except for a shallow layer of water covering the bottom of the tank.

Auxiliary tank

A second cylindrical plastic tank, located adjacent to the system tank and denoted here as the auxiliary tank, is initially filled with about 168 kg of tap water. The mass of water in this tank is determined by a differential weighing procedure via a scale with 0.1 kg resolution. This water mass is normally confirmed by measuring the volume of water in the tank by means of a flow meter, however, this device was found to be defective during the present tests so the water mass was determined by the mass scale reading alone. The temperature of the water in the auxiliary tank is adjusted to about 44°C by a small electric immersion heater. The water in the auxiliary tank is then pumped into the system tank, immersing the plasma cell (except for the glow discharge electrode), support structure, water jet pumps and various cables and gas feed lines.

Preheat phase

The preheating phase begins at time t_0 . At this time the liquid gallium flow through the cell is started by the EM pump and the plasma is initiated in the cell with a modest electrode power level of about 24 kW. A 2000 sccm flow of pure hydrogen is delivered to the cell and no glow discharge is used in the early stages of the preheat phase. Both water jet pumps in the bath are operated continuously. One of the pumps focuses a concentrated stream of water on the cell surface to prevent film boiling while the other concentrates a narrow jet of water on the glow discharge electrode (protruding above the bath free surface). Due to the electrode power input and modest plasma energy release during the early stages of the preheat phase, the bath water is heated by both convection and subcooled boiling at the cell surface. And because the bath water is well below the water saturation temperature, most of the generated vapor condenses before escaping from the bath surface. Nevertheless, vapor is continually lost from the bath free surface, and at an increasing rate as the bath temperature increases. The gallium temperature in the cell is monitored by a single thermocouple probe and the bath water temperature is monitored, similarly, by a single thermocouple probe immersed in the bath. At 1450 s into the preheat phase the electrode and EM pump power are both shut down in order to clean the filter upstream of the scroll vacuum pump which maintains the low (~ 5 Torr) pressure in the cell. The water jet pumps continue to operate during this shut-down period which is nominally 270 s in duration. At about 1720 s ($= 1450 \text{ s} + 270 \text{ s}$) power to the electrodes and the EM pump is resumed, however, the electrode power is now increased to about 36 kW. Also at this time the glow discharge is established in the cell and the hydrogen flow is increased to about 3000 sccm mixed with an additional 1 sccm of oxygen. These conditions further enhance the plasma power output as well as the cell and bath temperature. When the bath temperature reaches approximately 90°C both water jet pumps shut down owing to self-protection circuitry in the pumps. At this time vigorous nucleate boiling occurs at the cell surface and the correspondingly vigorous bubble release at the bath surface cools the glow discharge electrode by splash cooling,

ensuring that heat release from the electrode is re-captured by the bath. At about 2300 s into the preheat phase the bath temperature has nearly reached 100°C and the cell temperature is in the range 300-400°C. The preheat phase continues until time $t_1 = 2750$ s when the cell temperature may exceed 400°C. At this time the preheat phase of the test ends and the power phase begins.

Power phase

From time t_1 onward the plasma electrode current is maintained at 1.5 kA which results in variable electrode power between about 35 and 50 kW. The hydrogen flow is maintained at approximately 3000 sccm with 1 sccm of oxygen and the glow discharge is maintained with about 300 V. The electrode voltage and current are continuously recorded during the power phase with a sampling frequency of 20 kHz (one sample every 50 μ s). The voltage and current supplied to the EM pump and the glow discharge during the power phase are also noted, however, these parameters are known less precisely because the corresponding data are not recorded by the DAS. Also, the cell/gallium and bath temperatures are logged to computer memory once every second. During this period of strong cell heat release the bath water is nearly at 100°C so vigorous nucleate boiling occurs at the cell surface and most of the vapor generated escapes from the bath free surface. The power phase of the test run is terminated at time $t_2 = 2950$ s which corresponds to a power phase duration of 200 s. At this time electrode power to the cell ceases and power to the EM pump and the glow discharge is removed.

Post-power phase

After the power phase is complete, the water in the bath is pumped from the system tank back to the auxiliary tank without delay. Only the same small volume of water which was originally in the system tank is allowed to remain. The mass of water pumped into the auxiliary tank is weighed, differentially, by the same mass scale used previously. This water mass is compared to the mass initially pumped into the system tank and the difference is the mass of water lost as vapor during both the preheat and power phases of the test.

Control experiment

The vapor loss during the preheating phase is determined in a separate control experiment in which conditions are maintained nominally the same as those prevailing during the preheating phase. That is, the bath water temperature, electrode power and EM pump power are nominally the same as in the preheating phase. Further, the hydrogen/oxygen flow and the glow discharge operation during the control are adjusted to mimic operation during the preheat phase. Also, the 270 s shut down period for filter cleaning is included in the control experiment to match the procedure in the preheat phase. In this way the amount of vapor loss during the control experiment is very nearly the same as in the preheating phase. The mass of this vapor loss is easily determined at the conclusion of the control experiment by transferring the water to the auxiliary tank as described above.

Electrode and EMP power supplies, and instrumentation

Electrode power was supplied by a LabView-controlled switch mode rectifier (American CRS Q500 IP32), electrode voltage was monitored using a differential probe (PicoTech TA041, ± 70 V), and current was monitored by a DC Hall effect sensor (GMW CPCO-4000-77-BP10, ± 4 kA). Electrode voltage and current were sampled by a high-resolution oscilloscope (PicoScope 5000 Series) at 20 kHz sampling rate. The EMP was powered by a programmable DC power supply (Matsusada Precision REK10-1200) in current control mode. The resulting current and voltage supplied to the EMP was very stable and therefore these data were not saved by the DAS, but rather the mostly constant current and voltage were recorded manually. The glow discharge current and voltage were similarly monitored and manually recorded. The hydrogen (2000 or 3000 sccm) and oxygen (0 or 1 sccm) flows were controlled by separate mass flow controllers (MKS 1179A53CR1BVS for H₂ and MKS M100B12R1BB for O₂). The bath water jet pumps were Little Giant 5-MSP (1200 gph at 1 foot head, 125 W). The cell internal temperature was monitored by a K-type (ungrounded) thermocouple probe which extended about one cm into the gallium pool. Bath temperature was measured by a single thermocouple probe which was immersed in the bath several inches below the water surface, near the bath wall. The single probe for measuring bath temperature is thought to be sufficient since bath water temperature is spatially uniform (near 100°C) and varies temporally by only a fraction of a degree during the power phase. Cell temperature and bath temperature data were sampled at one second intervals and saved by the data acquisition system.

Energy conservation

The basis for applying energy conservation is a deformable, open thermodynamic system consisting of the water in the bath as well as the cell and related immersed components, e.g. the EMP, jet pumps, interconnecting power cables, etc. The energy conservation equation is derived in the report on the calorimetry tests conducted on November 10, 2020. After simplification, energy conservation applied to the power phase takes the form

$$E_{\text{Plasma}} = \left\{ \begin{array}{l} m_{w1}(h_{w2} - h_{w1}) - \delta m_w (h_{\text{vap}2} + (h_{v,\text{lost}} - h_{v2})) + \sum_j m_j (h_{j2} - h_{j1}) \\ -E_{\text{Elect}} - E_{\text{EMP}} - E_{\text{GD}} - [E_{\text{WJ}} - Q_{\text{Loss}}] - \sum_{\text{H}_2, \text{H}_2\text{O}} m(h_i - h_e) \end{array} \right\}$$

where E and h denote energy and specific enthalpy, m_{w1} and δm_w are the mass of water in the bath at time t_1 and the change in mass during the time interval $t_1 < t < t_2$, and $h_{\text{vap}2}$ is the enthalpy of vaporization and h_{v2} is the enthalpy of saturated vapor, each at the bath temperature at the end of the power phase (time t_2). The enthalpy $h_{v,\text{lost}}$ is the specific enthalpy of the vapor lost from the bath surface during the process. The final summation is the net enthalpy entering the bath due to the gas through-flow. The electrode, EM pump and glow discharge energy terms are the integrated power inputs during the power phase

$$E_{\text{Elect}} = \int_{t_1}^{t_2} P_{\text{Elect}} dt, \quad E_{\text{EMP}} = \int_{t_1}^{t_2} P_{\text{EMP}} dt, \quad E_{\text{GD}} = \int_{t_1}^{t_2} P_{\text{GD}} dt$$

and the m_j and h_j denote the masses and specific enthalpies of the various components in the bath such as the cell parts, the gallium working fluid, the EM pump, the water jet pumps, etc. The corresponding thermal mass data are tabulated in Table 1.

Table 1. Component masses, specific heats and thermal masses

	Material	m_j [kg]	C_{p_j} [kJ/kg-K]	$m_j C_{p_j}$ [kJ/K]
Main cell body with flanges	Stainless/Cr-Mo	12.9	0.46	5.934
Lower cell body (4 inch) with base	Cr-Mo	0.6	0.44	0.264
Carbon liner	Carbon	2.2	0.7	1.54
Niobium liner	Niobium	2.2	0.27	0.594
Tungsten liner	Tungsten	3.8	0.13	0.494
Copper bus bar	Copper	0.5	0.39	0.195
Tungsten bus bar	Tungsten	1	0.13	0.13
Glow discharge flanges and tube	Stainless	0.9	0.46	0.414
Gas evacuation tube	Stainless	0.25	0.46	0.115
Miscellaneous metal tubing	Stainless	0.3	0.46	0.138
Support standoffs	Stainless	0.5	0.46	0.23
Miscellaneous hardware	Stainless	1	0.46	0.46
EM pump magnet	Sm/Co	2.2	0.38	0.836
Gallium	Gallium	6	0.37	2.22
Water jet pump (2)	Steel	8	0.43	3.44
Connecting wire	Copper	1	0.39	0.39
Hose/conduit/insulation	Rubber	0.5	0.2	0.1
Totals		43.85		17.49

The energy contribution due to the hydrogen and water vapor flow through the cell is shown in Appendix 1 to be on the order of only 1 kJ, which is negligible compared to other energy terms in the balance, so it is ignored. Also, the term $E_{\text{WJ}} = 0$ since both water jet pumps shut down prior to the start of the power phase at time t_1 . The term Q_{Loss} is the heat loss from the bath by heat convection and conduction to the lab, estimated from a measurement of bath temperature decay for bath temperatures between about 85 and 96°C, cf. Appendix 2. The rate of heat loss is found to be about 2.4 kW. This estimate is thought to have an uncertainty as large as $\pm 50\%$ for reasons discussed in Appendix 2. Also, the difference $h_{v,\text{lost}} - h_{v2}$, which is the difference between the enthalpy of the vapor leaving the bath surface and the enthalpy of saturated vapor at the final bath temperature, is almost zero because the bath temperature during the power phase is nearly 100°C. In any case this difference is completely negligible compared with the enthalpy of vaporization $h_{\text{vap}2}$. With these simplifications the plasma energy release in the power phase reduces to

$$E_{\text{Plasma}} = m_{w1}(h_{w2} - h_{w1}) - \delta m_w h_{\text{vap}2} + \sum_j m_j (h_{j2} - h_{j1}) + Q_{\text{Loss}} - E_{\text{Elect}} - E_{\text{EMP}} - E_{\text{GD}} \quad (1)$$

where it is also noted that the change in bath water mass $\delta m_w < 0$, so vaporization corresponds to a positive contribution to E_{Plasma} .

Control experiment

A single control experiment was conducted to determine the vapor loss during the preheat phase in both of the calorimetric tests (Run 1 and Run 2). The control experiment began with 167.7 kg of water added to the system tank. Both the cell and bath temperature were in the range 43-44°C at the start of the control. The plasma cell was operated for 1450 s before system shut down for cleaning the gas filter. During this pre-shut down period the electrode and EMP power levels were moderate, pure hydrogen flowed through the system at 2000 sccm, and the glow discharge was powered off. During the 270 s shut down all devices were powered off except the water jet pumps. After re-starting at 1720 s, the electrode and EMP power were increased, the glow discharge was powered on, and gas flow was increased with trace oxygen added to the hydrogen flow. The control experiment was terminated at 2750 s. During the control the pressure in the cell was about 5 Torr, except during the shut down period. The nominal values of the system parameters during the various phases of the control experiment are summarized in Table 2.

Table 2. Control experiment summary

Pre shut-down operation	
Electrodes:	1 kA; 24 V; 24 kW
EMP:	250 A; 0.35 V; 87.5 W
GD:	Off
Gas flow:	2000 sccm H ₂
WJ pumps:	Running
Filter shut-down:	1450 s
Shut down interval:	270 s
Restart:	1720 s
Post re-start operation	
Electrodes:	1.5 kA; 24 V; 36 kW
EMP:	500 A; 0.8 V; 400 W
GD:	2 A; 135 V; 270 W
Gas flow:	3000 sccm H ₂ + 1 sccm O ₂
WJ pumps:	Running for T _{Bath} < 90°C
Control end:	2750 s

The cell/gallium and bath water temperature histories for the control experiment are plotted in Fig. 2. The cell temperature increased rapidly during the initial phase of the control due primarily to electrode power and probably some power release by the plasma. The gallium temperature increased to about 300°C and remained near that level until the shut down at 1450 s. The bath water temperature increased mostly linearly, reaching about 85°C at the time of shut-down. During the 270 s shut down period the cell cooled very quickly to ~104°C due to convective heat loss and phase change at the cell exterior surface. The bath temperature reduced only about 0.1°C during the shut down. When the electrode and EMP power was restarted and

the glow discharge was powered on, the cell temperature quickly recovered, averaging near 380°C from about 2100 s to the end of the control test at 2750 s. The bath water temperature rose mostly linearly from the restart until about 2300 s at which time the bath water was essentially at 100°C. After reaching this temperature, vigorous and mostly saturated nucleate boiling occurred at the cell surface until the end of the control.

The cell and bath temperature behaviors plotted in Fig. 2, taken together, infer the rate of vapor loss from the bath at each time. Very high cell surface temperature or very high bath temperature do not necessarily indicate a high rate of vapor loss. Rather, it is high cell surface temperature in excess of the water saturation temperature coupled with bath temperature near saturation which results in rapid vapor bubble formation at the cell and low condensation during bubble rise in the bath liquid. These conditions, when present simultaneously, result in a high rate of vapor loss from the bath. For this reason the cell and bath temperature histories during the preheat phase of the calorimetric tests will be compared with the corresponding histories during the control. If the temperature histories coincide for the preheat phase and the control, then it is reasonable to conclude that the water mass boil-off during the preheat and the control are the same.

Soon after power shut down in the control experiment, the water was pumped back into the auxiliary tank and weighed. In this process, vapor rising off the water surface was allowed to condense and then was directed back into the tank. The water mass added to the auxiliary tank was found to be 157.4 kg. Therefore, the mass loss due to vaporization in the control experiment was $167.7 - 157.4 = 10.3$ kg.

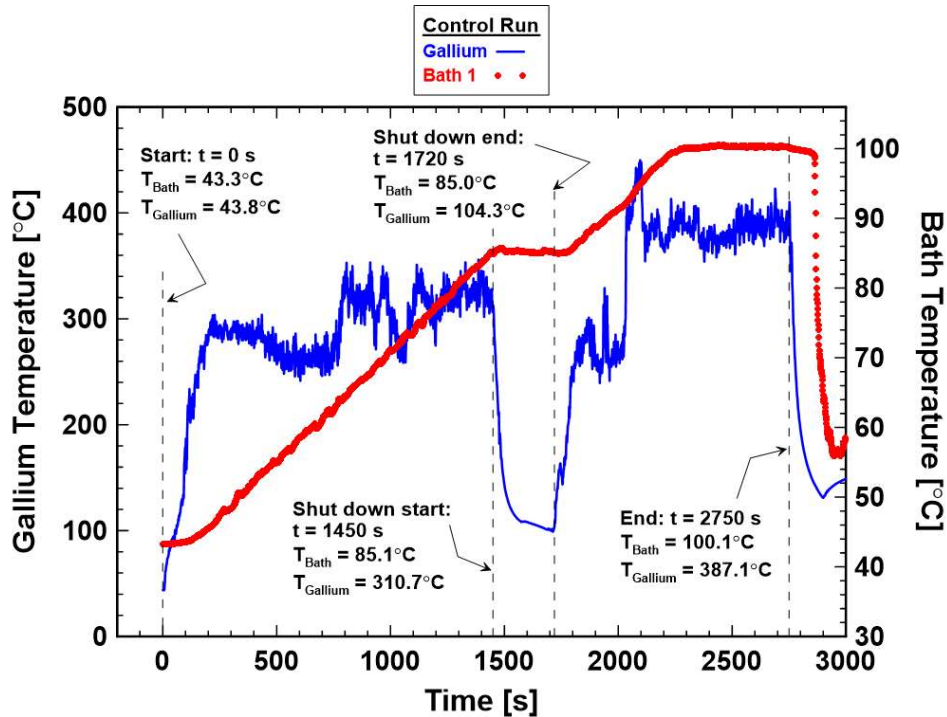


Figure 2. Cell and bath temperature histories in control experiment

Calorimetric Run 1

This test was conducted with a preheat phase to bring the cell up to optimal operating temperature, followed by a power phase in which the plasma power was measured. Pressure in the cell was about 5 Torr during the run, except during the shut down in the preheat phase.

Preheat phase

Run 1 began with 167.7 kg of water in the system tank, the same mass as in the control experiment. Both the cell and bath water were about 44°C at the start of the test. During the preheat phase conditions were maintained similar to those present during the control experiment, compare Tables 2 and 3. However, at the end of the shut down for filter cleaning the glow discharge failed to operate, probably because of shorting between the glow discharge electrode and the immediately adjacent cell structure. Efforts to revive the glow discharge were unsuccessful so the re-start began at 1843 s without a glow discharge. The shut down period lasted 393 s or about 123 s longer than the standard 270 s shut down period used in the control, cf. Table 3. Except for the absence of the glow discharge, the system parameters during the post-restart period were similar to the control, cf. Tables 2 and 3. This period of operation continued until $t_1 = 2873$ s, therefore the post-shut down period of the preheat phase continued for $2873 - 1843 = 1030$ s, the same as in the control.

Table 3. Run 1 preheat phase summary

Pre shut-down operation	
Electrodes:	1 kA; 24 V; 24 kW
EMP:	250 A; 0.36 V; 90 W
GD:	Off
Gas flow:	2000 sccm H ₂
WJ pumps:	Running
Filter shut-down:	1450 s
Shut down interval:	393 s
Restart:	1843 s
Post re-start operation	
Electrodes:	1.5 kA; 24 V; 36 kW
EMP:	411 A; 0.65 V; 267 W
GD:	Off
Gas flow:	4000 sccm H ₂ + 1 sccm O ₂
WJ pumps:	Running for T _{Bath} < 90°C
End preheat phase:	2873 s

The gallium and bath water temperature in Run 1 are plotted in Fig. 3. The bath and gallium temperatures in the control are also plotted there, for comparison. The cell and bath temperature behaviors during the pre- and post-shut down periods are very similar for Run 1 and the control, and the durations of these two periods are also the same for Run 1 and the control. [The similarity of temperatures is best observed by translating the post-restart data for Run 1 backward in time by 123 s, the difference in duration for the shut down in Run 1 and the control.] The similarity suggests that vapor loss from the bath during the pre- and post-shut down periods is about the same in Run 1 and the control. However, the shutdown period is 123 s longer in Run 1, during which time vapor loss from the bath continued. The contribution to the total vapor loss from this 123 s period is expected to be relatively small because the cell temperature is quite low and the bath temperature is well below saturation during the shut down. Hence, the vapor boil-off during the preheat phase of Run 1 can reasonably be assumed equal to the boil-off in the control, that is, 10.3 kg. This assumption is critical for the efficacy of the two-phase calorimetry approach used here.

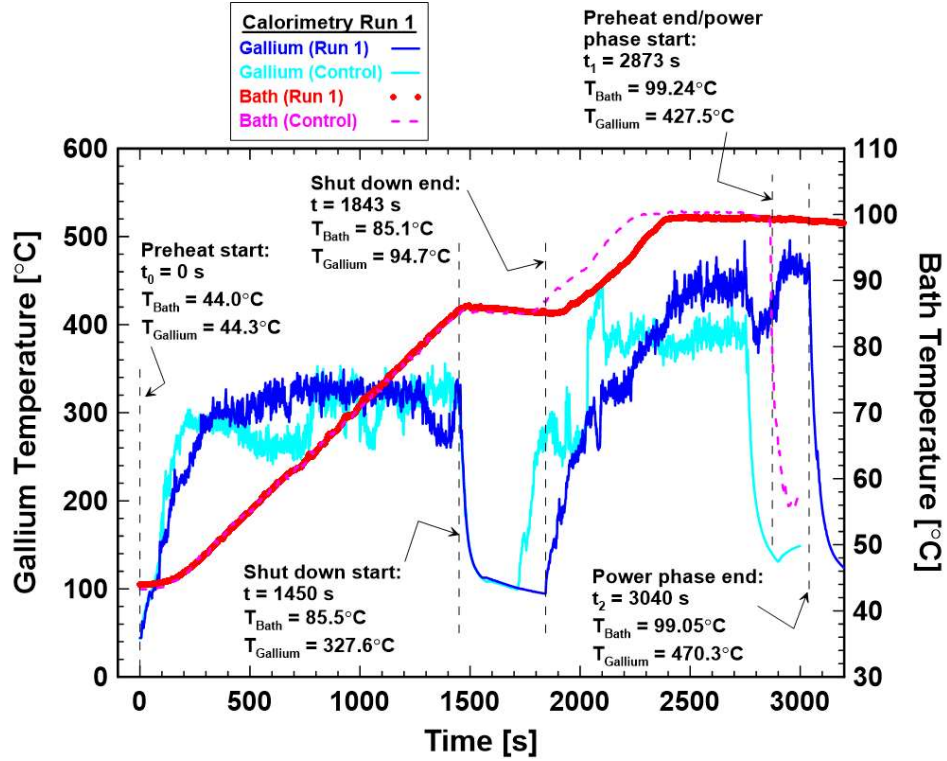


Figure 3. Cell and water bath temperature history in Run 1

Power phase

The power phase began at time $t_1 = 2873$ s at which time the cell and bath temperatures were about 428 and 99°C. During the 167 s long power phase the EMP and glow discharge power levels were maintained similar to the post-restart period of the preheat phase: $P_{EMP} = 271$ W, $P_{GD} = 0$. The cell temperature averaged about 460°C during the power phase while the bath temperature was mostly constant near 99°C. During this period most of the heat transferred from the cell results in vapor loss from the bath due to vigorous saturated boiling.

The voltage, current and power variations at the electrodes during the power phase are plotted in Figs. 4 and 5. These plots were constructed by combining four separate files of V, I and VI data, spanning approximately 50 seconds each. The voltage, current and power could not be plotted on the same coordinates because the very large number of data records, due to the 20 kHz sampling rate, exceeded computer memory. Also note that the time coordinate in the V, I and VI plots is independent of the time coordinate used in the temperature plot for Run 1. In any case, the power phase is identified in Figs. 4 and 5 from the time that power is shut off, 191.7 s, and the 167 s duration of the power phase. This results in the power phase start at 24.7 s. During the power phase the current is stable near 1.5 kA while the voltage varies modestly between about 24 and 35 V. The power varies in the range from about 36 to 50 kW. During the 167 s power

phase the time-integrated electrode power was determined by trapezoid integration to be $E_{\text{Elect}} = 6950.7 \text{ kJ}$, cf. Fig. 5.

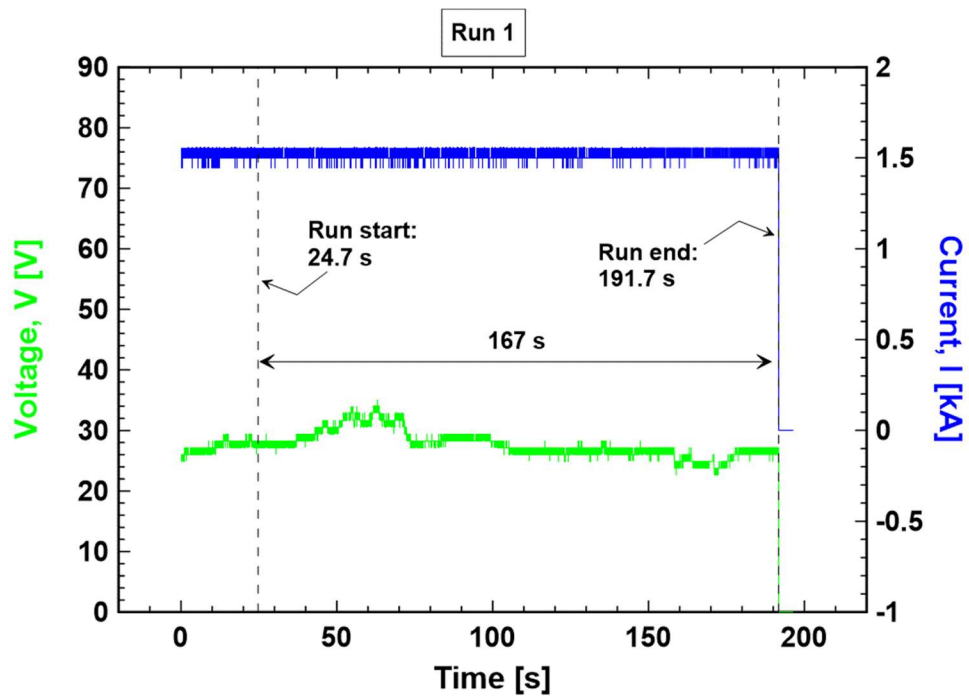


Figure 4. Electrode voltage and current history during Run 1 power phase

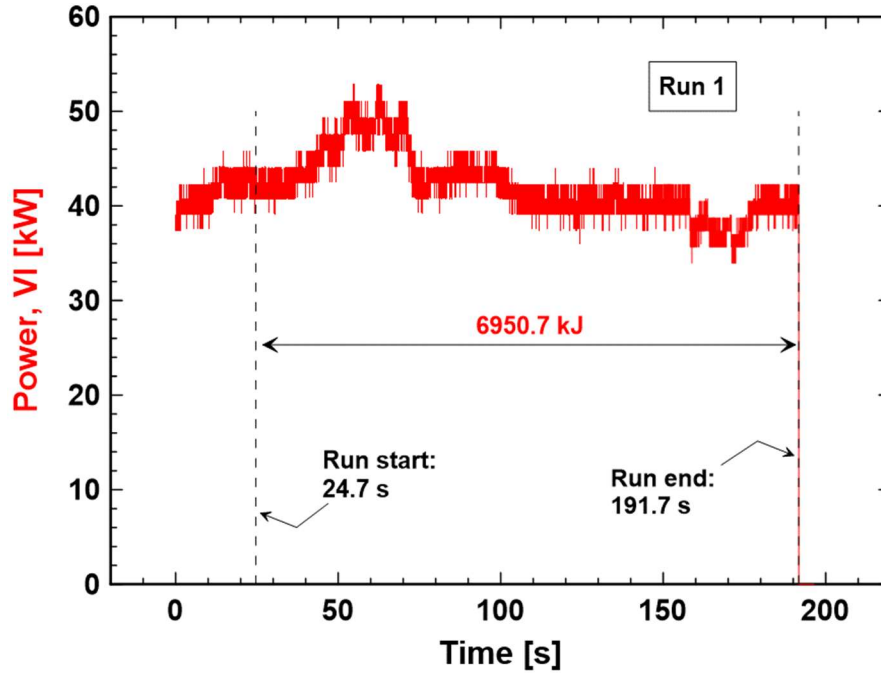


Figure 5. Electrode power history during Run 1 power phase

After the power phase ended the mass of water in the system tank was transferred to the auxiliary tank and weighed. The mass of the transferred water was 150.3 kg, therefore $167.7 - 150.3 = 17.4$ kg of water was boiled off during the preheat and power phases of Run 1. And, using the 10.3 kg boil-off from the control, the amount boiled off during the power phase was about $17.4 - 10.3 = 7.1$ kg. This, along with the very slight bath water temperature fall during the power phase and the energy inputs due to electrode and EMP power results in the energy values tabulated in Table 4. The greatest contributors to the energy balance are the energy of vaporization (16,046 kJ) and the electrode energy (6951 kJ). A small sensible heat loss (-134 kJ) occurs because of the small decrease in bath temperature during the power phase. The plasma energy is found from Eq. (1) to be about 9313 kJ which corresponds to an average plasma power of 55.8 kW during the 167 s power phase. The gain is

$$\text{Gain} = (E_{\text{Plasma}} + E_{\text{Elect}}) / E_{\text{Elect}} = 2.34$$

which indicates that the plasma energy release is about 134% of the plasma maintenance energy.

Table 4. Energy results data for Run 1

m_{w1} [kg]	167.7	C_{pw} [kJ/kg-K]	4.217	P_{EMP} [kW]	0.271
δm_w [kg]	-7.1	h_{vap2} [kJ/kg]	2260	P_{GD} [kW]	0
$\Delta t = t_2 - t_1$ [s]	167	$\Sigma m_j C_{pj}$ [kJ/K]	17.49	Heat loss rate [kW]	2.4
$\Delta T = T_2 - T_1$ [K]	-0.19				
$m_{w1} C_{pw} \Delta T$ [kJ]	-134.4	E_{Plasma} [kJ]	9313.2		
$\delta m_w h_{vap2}$ [kJ]	-16046.0	Gain [1]	2.340		
$\Sigma m_j C_{pj} \Delta T$ [kJ]	-3.32	P_{Plasma} [kW]	55.767		
Q_{Loss} [kJ]	400.8				
E_{Elect} [kJ]	6950.7				
E_{EMP} [kJ]	45.3				
E_{GD} [kJ]	0.0				

Uncertainties in the plasma energy result principally from uncertainties in measuring the boil-off mass δm_w and the estimate of heat loss rate from the bath. Uncertainty in δm_w of ± 0.1 kg results in changes to the calculated plasma energy of about 2.4%. And, variations in plasma energy of about 2.2% arise from the $\pm 50\%$ uncertainty in the heat loss estimate.

Calorimetric Run 2

As in Run 1, this test was conducted with a preheat phase to bring the cell up to optimal operating temperature, followed by the power phase. Pressure in the cell was about 5 Torr during Run 2, except for the shut down in the preheat phase.

Preheat phase

Run 2 also began with 167.7 kg of water in the system tank. At the start of the preheat phase the cell and bath temperatures were about 44 and 45.5°C, very close to the starting values in the control. And, during the preheat phase conditions were maintained very near to those used in the control experiment, compare Tables 2 and 5. In Run 2, unlike Run 1, the shut down was of the same duration as in the control (270 s) and the glow discharge operated normally after the shut down. However, the post-shut down EMP and glow discharge power levels were lower in Run 2 than in the control experiment. This post-shut down period of operation continued until 2750 s. Therefore the post-shut down period of the preheat phase had a duration of 1030 s, the same as in the control.

Table 5. Run 2 preheat phase summary

Pre shut-down operation	
Electrodes:	1 kA; 24 V; 24 kW
EMP:	230-300 A; 0.35 V; 81-105 W
GD:	Off
Gas flow:	2000 sccm H2
WJ pumps:	Running
Filter shut-down:	1450 s
Shut down interval:	270 s
Restart:	1720 s

Post re-start operation	
Electrodes:	1.5 kA; 24 V; 36 kW
EMP:	400 A; 0.6 V; 240 W
GD:	0.47 A; 290 V; 136 W
Gas flow:	3000 sccm H ₂ + 1 sccm O ₂
WJ pumps:	Running for T _{Bath} < 90°C
End preheat phase:	2750 s

The gallium and bath water temperature in Run 2 are plotted in Fig. 6 along with the bath and gallium temperatures in the control experiment, for comparison. The bath temperature in Run 2 closely tracks the temperature in the control, exceeding the temperature in the control by no more than about 3°C. The cell temperature during the pre-shut down period is very nearly the same as in the control and during the post-shut down period the cell temperature is, on average, somewhat lower than in the control. However, this difference results in lower vapor loss in Run 2 during the preheat phase compared to the control, which serves to reduce the calorimetric estimate of plasma energy release. Aside from this difference, the vapor boil-off during the preheat phase of Run 2 can reasonably be assumed equal to the boil-off in the control, that is, 10.3 kg.

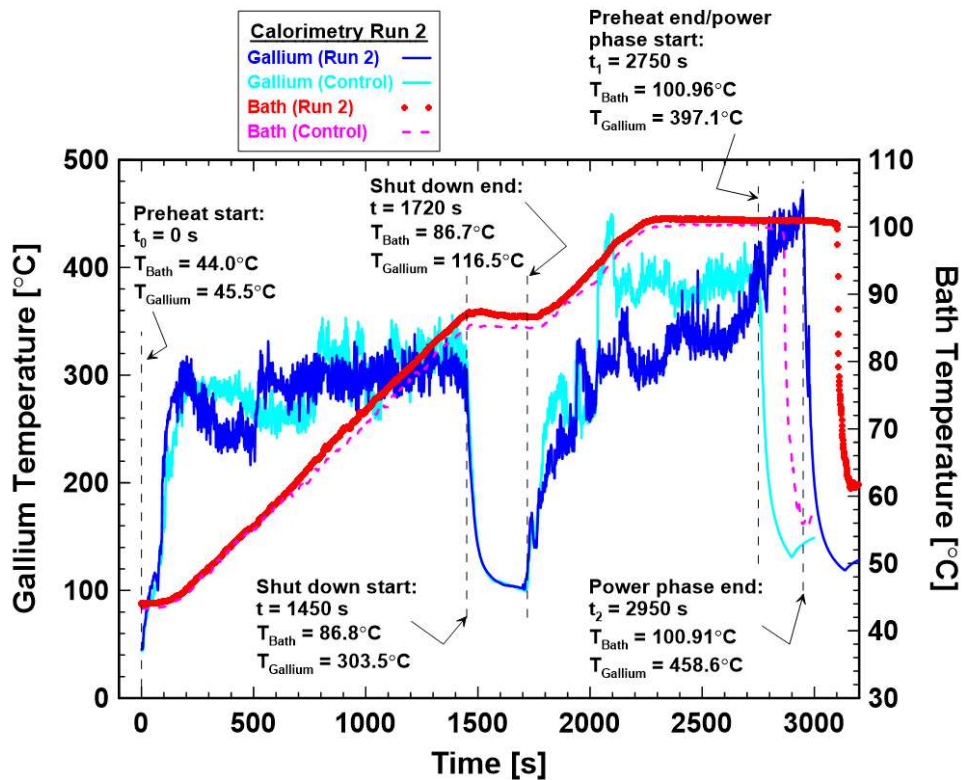


Figure 6. Cell and water bath temperature history in Run 2

Power phase

The power phase began at 2750 s at which time the cell and bath temperatures were about 397 and 100°C. The recorded bath temperature of 101°C is due to a small calibration error in the bath temperature thermocouple probe. During the 200 s long power phase the EMP and glow discharge power levels were maintained at similar levels to the post-restart period of the preheat phase: $P_{EMP} = 284$ W, $P_{GD} = 118$ W. The cell temperature averaged about 425°C during the power phase while the bath temperature was mostly constant near 100°C. Note, the important difference in Run 2 relative to Run 1 is that the glow discharge was present during the power phase of Run 2.

The voltage, current and power variations at the electrodes during the power phase are plotted in Figs. 7 and 8. These plots were constructed by combining five separate files of V, I and VI data, spanning approximately 50 seconds each. Also note that the time coordinate in the V, I and VI plots is independent of the time coordinate used in the temperature plot for Run 2. In any case, the power phase is identified in Figs. 7 and 8 from the time that power is shut off, 245.0 s, and the 200 s duration of the power phase. This results in the power phase start at 45.0 s. During the power phase the current is stable near 1.5 kA while the voltage varies modestly between about 23 and 27 V. The power varies in the range from about 32 to 44 kW. During the 200 s power phase the time-integrated electrode power was determined by trapezoid integration to be $E_{Elect} = 7799.5$ kJ, cf. Fig. 8.

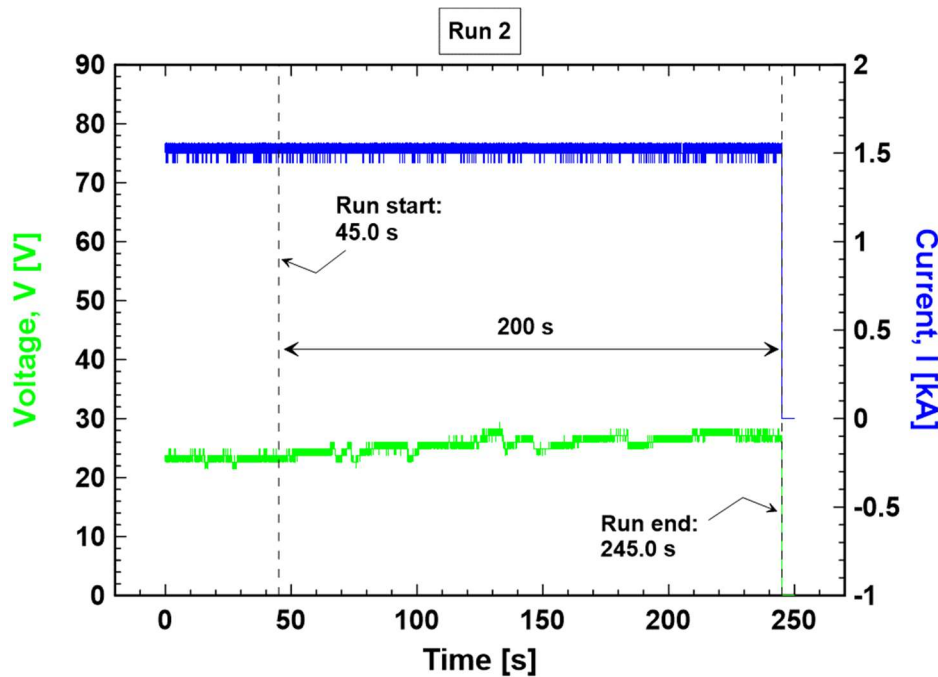


Figure 7. Electrode voltage and current history during Run 2 power phase

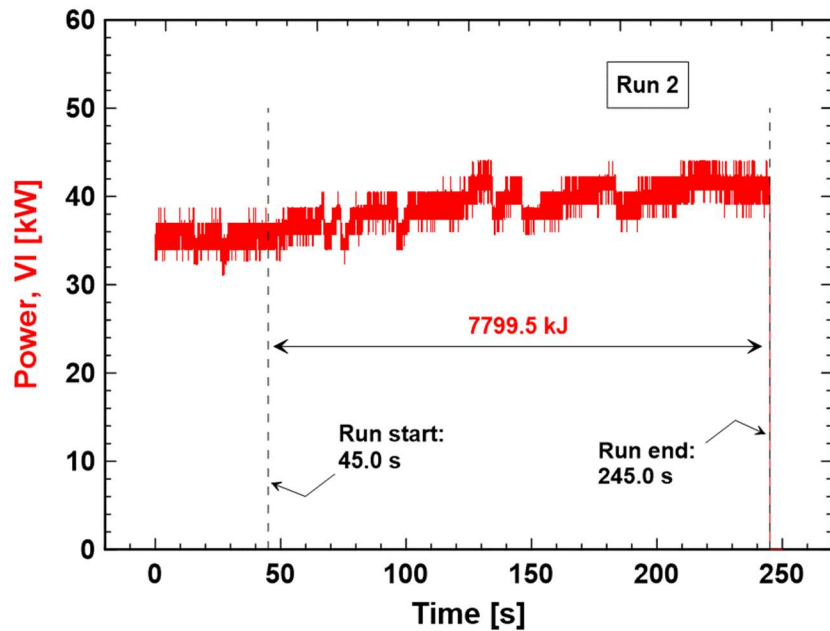


Figure 8. Electrode power history during Run 2 power phase

After the power phase ended, the mass of water in the system tank was transferred to the auxiliary tank and weighed. The mass of the water transferred to the auxiliary tank was 145.9 kg. Therefore, the vaporization mass loss in Run 2 was $167.7 - 145.9 = 21.8$ kg, and correcting for vaporization during the preheat phase the net vapor loss during the power phase was 11.5 kg. These data are used in Table 6 to calculate the various energy flows in Run 2. Similar to Run 1, the greatest contributors to the energy balance are the energy of vaporization (25,956 kJ) and the electrode energy input (7800 kJ). The plasma energy is found to be about 18,592 kJ which corresponds to an average plasma power of 93 kW during the 200 s power phase. The gain is

$$\text{Gain} = (E_{\text{Plasma}} + E_{\text{Elect}}) / E_{\text{Elect}} = 3.38$$

indicating that the plasma energy release is 238% of the plasma maintenance energy during the power phase. Uncertainties in the plasma energy due to uncertainties in the measured boil-off mass and the heat loss from the bath are only about 1.3%.

Table 6. Energy results data for Run 2

m_{w1} [kg]	167.7	C_{pw} [kJ/kg-K]	4.217	P_{EMP} [kW]	0.284
δm_w [kg]	-11.5	h_{vap2} [kJ/kg]	2257	P_{GD} [kW]	0.118
$\Delta t = t_2 - t_1$ [s]	200	$\sum m_j C_{pj}$ [kJ/K]	17.49	Heat loss rate [kW]	2.4
$\Delta T = T_2 - T_1$ [K]	0.05				
$m_{w2} C_{pw} \Delta T$ [kJ]	35.4	E_{plasma} [kJ]	18591.8		
$\delta m_w h_{vap2}$ [kJ]	-25955.5	Gain [1]	3.384		
$\sum m_j C_{pj} \Delta T$ [kJ]	0.87	P_{plasma} [kW]	92.959		
Q_{Loss} [kJ]	480.00				
E_{elect} [kJ]	7799.5				
E_{EMP} [kJ]	56.8				
E_{GD} [kJ]	23.6				

Appendix 1. Enthalpy transfer due to gas flow

The enthalpy transfer into the bath due to hydrogen and water vapor flow is

$$\sum_{H_2, H_2O} m(h_i - h_e)$$

Ignoring the very small contribution due to the water vapor formed from the 1 sccm of oxygen combining with the excess hydrogen, the enthalpy transfer becomes

$$m_{H_2} C_{pH_2} (T_i - T_e)$$

where m_{H_2} is the total mass of hydrogen which flows through the cell during the interval $t_1 < t < t_2$, T_i is the gas temperature entering the bath and T_e is the gas temperature leaving the bath. Assuming hydrogen flow at 3000 sccm for 5 minutes the total mass is

$$15,000 \text{ scc} \times \frac{1 \text{ mol } H_2}{22,400 \text{ scc}} \times \frac{2.016 \text{ g}}{1 \text{ mol } H_2} = 1.35 \text{ g } H_2$$

so the enthalpy transfer is

$$m_{H_2} C_{pH_2} (T_i - T_e) = 0.0014 \text{ kg} \times 14.21 \text{ kJ/kg-K} \times (25^\circ\text{C} - 97.5^\circ\text{C}) = -1.44 \text{ kJ}$$

Appendix 2. Estimate of heat loss rate

A supplemental experiment was conducted with the system tank filled with 185.7 kg of water and all normal components in place. The bath was heated to about 96°C and then allowed to cool without water jet agitation. The bath temperature change over a period of about 4000 s is shown in Fig. A2.1.

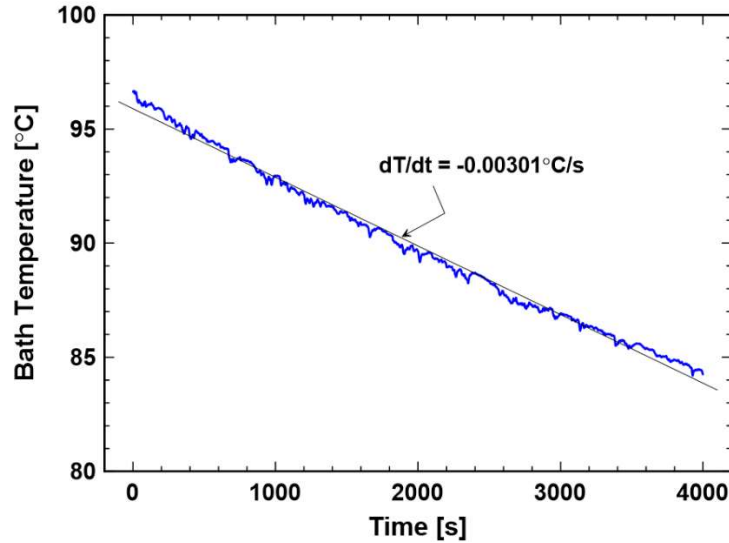


Figure A2.1. Bath cooling without agitation

The rate of heat loss from the tank is approximately

$$\dot{Q}_{\text{Loss}} = \left[m_w C_{pw} + \sum_j m_j C_{pj} \right] \left(-\frac{dT}{dt} \right)_{\text{Bath}}$$

where the temperatures of the various thermal masses in the tank such as the cell, EM pump, etc. are assumed to track the bath water temperature. Using the water mass, $m_w = 185.7$ kg, $\sum_j m_j C_{pj} = 14.87$ kJ/K and the measured time rate of temperature change results in

$$\dot{Q}_{\text{Loss}} = 2.4 \text{ kW}$$

This is a very crude estimate of the loss rate during the power phase, for many reasons. The actual temperature of the bath during a run is very close to 100°C, which would result in slightly greater heat loss than in this supplemental experiment. Conversely, the data in Fig. A2.1 may

overestimate the rate of temperature decay because the bath temperature transducers may be sensing locally depressed temperature in the mostly cooler thermal boundary layer near the bath walls. During an actual run the very vigorous boiling at the cell ensures that the water is well-mixed. Also, for bath water temperature near saturation, evaporative cooling of the water at the surface plays a larger role and this may be affecting the measured rate of temperature change in Fig. A2.1. This mode of energy transfer is distinct from sensible heat loss and is already accounted for via the enthalpy of vaporization term in the energy balance. The estimate of 2.4 kW may have an uncertainty as large as $\pm 50\%$.